

# Zero-to-Hero: Zero-Shot Initialization Empowering Reference-Based Video Appearance Editing

Tongtong Su<sup>1,2</sup>, Chengyu Wang<sup>2\*</sup>, Jun Huang<sup>2</sup>, Dongming Lu<sup>1\*</sup>

<sup>1</sup> Zhejiang University, <sup>2</sup> Alibaba Cloud Computing

{sutongtong, ldm}@zju.edu.cn,

{chengyu.wcy, huangjun.hj}@alibaba-inc.com

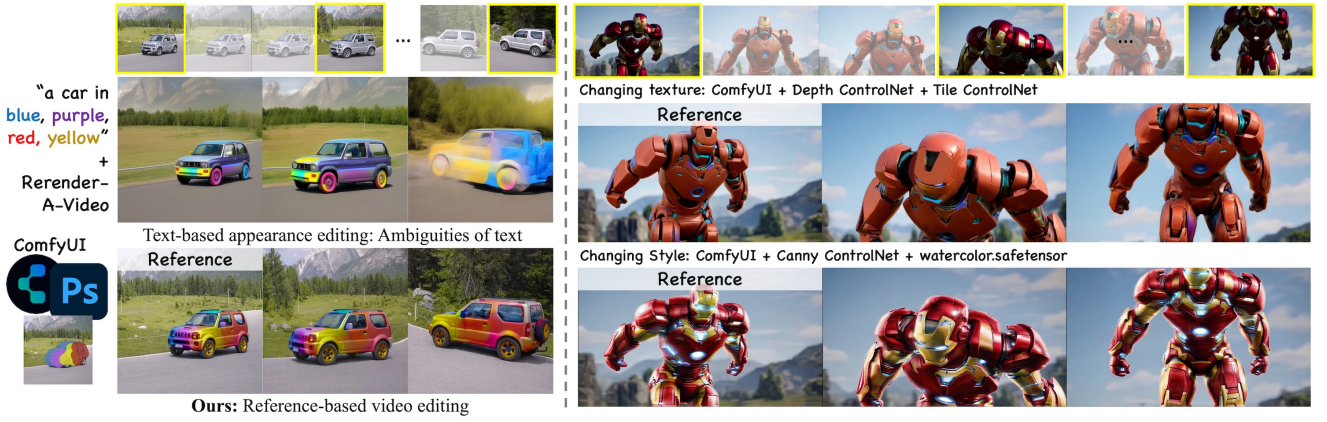


Figure 1. **Left:** Our reference-based editing method enables users to precisely edit appearances by incorporating complex layouts of color with arbitrary tools such as Photoshop or ComfyUI to create references, then consistently propagate these edits to subsequent frames. **Right:** Our approach supports all spatially-aligned appearance editing, including texture and style.

## Abstract

Appearance editing according to user needs is a pivotal task in video editing. Existing text-guided methods often lead to ambiguities regarding user intentions and restrict fine-grained control over editing specific aspects of objects. To overcome these limitations, this paper introduces a novel approach named Zero-to-Hero, which focuses on reference-based video editing that disentangles the editing process into two distinct problems. It achieves this by first editing an anchor frame to satisfy user requirements as a reference image and then consistently propagating its appearance across other frames. We leverage correspondence within the original frames to guide the attention mechanism, which is more robust than previously proposed optical flow or temporal modules in memory-friendly video generative models, especially when dealing with objects exhibiting large motions. It offers a solid ZERO-shot ini-

tialization that ensures both accuracy and temporal consistency. However, intervention in the attention mechanism results in compounded imaging degradation with over-saturated colors and unknown blurring issues. Starting from Zero-Stage, our Hero-Stage Holistically learns a conditional generative model for vidEo RestOration. To accurately evaluate the consistency of the appearance, we construct a set of videos with multiple appearances using Blender, enabling a fine-grained and deterministic evaluation. Our method outperforms the best-performing baseline with a PSNR improvement of 2.6 dB. The project page is at <https://github.com/Tonniia/Zero2Hero>.

## 1. Introduction

Video editing aims to modify the target video according to user demands. One of the most important sub-tasks is appearance editing [37, 40, 41], in which we preserve the structure of the target video frames while altering the color, texture of the object, or overall style. Previously,

\*Co-corresponding authors.

text-guided video editing addressed this task by leveraging pre-trained Text-to-Image (T2I) models, which rely on textual input (i.e., prompts) as the editing guidance signal [7, 9, 10, 13, 37, 40, 41]. However, ambiguities in text regarding user intentions may limit fine-grained control over the editing results. Therefore, a more practical solution for users to effectively convey their intentions is to explicitly provide a reference image, leading to the *reference-based video editing* task [15, 17, 24]. It disentangles video editing into two problems: (1) editing a single image as a reference and (2) consistently propagating it to subsequent frames.

The first sub-task can be addressed using T2I models or arbitrary user manipulation through art design software, allowing for fine-grained appearance changing. The main difficulty lies in the second sub-task: *how to consistently propagate the edited reference frame to other frames*. Current propagation methods can be divided into two groups. The first group of methods uses optical flow obtained from the target video to guide the propagation of reference image features [7, 40, 41]. The performance of these methods can be limited by optical flow estimation [38], which was trained on a specific set of videos. Consequently, its accuracy noticeably degrades when dealing with videos involving significant motion. The second group [15, 17, 24] leverages Image-to-Video (I2V) models [4, 46] to invert the target video to noisy latent representations, then uses the reference image as a guidance signal to denoise. However, the video length is constrained by the memory demands of inversion, and the temporal modeling limitations of these memory-friendly I2V models also restrict the range of motion. Recent work [24] fine-tunes the I2V model with specific target videos. However, for videos with significant motion that deviate far from the I2V domain, it is challenging to strike a balance between adequately fitting the motion pattern and preventing overfitting its appearance.

In this work, we explore propagation-based methods but redefine the propagation problem as the more general appearance transfer task [21, 25, 35]: maintaining the structure of the target image while utilizing the appearance of the reference image. This task involves finding the correspondence between reference and target images and then propagating the reference image features into the target ones. Recent approaches connect this task with the self-attention (SA) mechanism in diffusion models [8, 21, 22], leveraging their generative capabilities to support zero-shot appearance transfer. Diffusion models can inherently model intra-similarity for correspondence and simultaneously propagate features using SA. Given two images, expanding SA to cross-image attention (CiA) is a common method for fusing features between images [2, 6, 34]. However, basic CiA can only capture coarse-grained correspondence, as the query of the target image exhibits similarity to many keys in the ref-

erence image [2]. The weighted averaging of matched values leads to a loss of fine-grained details and limits the ability to handle fine-grained appearance transfer. Directly applying contrast value to the attention map can introduce inaccurate transfer since the attention map at the early denoising stage, with a high noise level, cannot represent accurate correspondence. Some research [20, 33, 44] has found that Diffusion FeaTures (DIFT) at certain timesteps and U-Net layers can best represent correspondence.

Obtaining correspondence is merely the first step. Directly performing pixel-level swapping based on the highest similarity without introducing a generative process remains highly sensitive to occasional inaccurate matching, often leading to artifacts, prominently marked by noticeable patch splitting [44]. Using correspondence to guide CiA during denoising is more robust, given the output domain constraint of the generative model. This is implemented through an attention mask, i.e., setting the top- $k$  entries in correspondence to 1 to construct the mask. When  $k = h \times w$ , it is the basic CiA, facing the same problem of weighted averaging of values from the reference. With gradually decreasing  $k$ , the transfer becomes more accurate. However, this also progressively over-intervenes in the attention maps, leading to a compounded degradation of over-saturated colors and blur patterns of unknown origin [1, 16]. There exists an upper limit to what can be achieved with zero-shot methods.

In this paper, we propose *Zero-to-Hero*, which builds upon the aforementioned ZERO-shot intermediate result (i.e., Zero-Stage) as a good initialization and incorporates the Hero-Stage for Holistic vidEo RestOration. This approach can be formulated as a conditional generation problem [45], where the training data pairs require ground truth. The sole ground truth available is the reference on the anchor frame. We observed that the Zero-Stage exhibits a similar pattern of degradation across all frames, indicating that training on the anchor frame has the potential to generalize effectively to all subsequent frames. To accelerate training convergence, the original frame is utilized as an auxiliary condition to encourage shortcut mapping for non-edited regions. To evaluate appearance consistency more accurately beyond semantic-level CLIP-based scores [12], we collect a set of 3D objects with multiple appearances and render them under significant camera motion to construct videos using *Blender*. This supports fine-grained and deterministic evaluation. Our method outperforms the best-performing baseline with a PSNR improvement of 2.6 dB.

## 2. Related Work

**Reference-based Video Appearance Editing.** Text-guided video editing addresses this task by leveraging pre-trained Text-to-Image (T2I) models, which rely on textual input (i.e., prompts) as the editing guidance signal [10, 37, 40,

41]. However, ambiguities in text regarding user intentions may limit fine-grained control over the editing process. Therefore, a more practical solution for users to effectively express their intentions is to use a single image, leading to *reference-based video editing* [15, 17, 24], which offers a more flexible solution for video editing. AnyV2V [15] adopts the earlier memory-friendly I2V model, I2VGen [46], for DDIM inversion [30]. During the denoising steps, intermediate features are selectively injected to preserve the original motion. This process requires fine-grained hyperparameter tuning of different injection rates at both spatial and temporal modules. Instead of relying on the original temporal module, I2VEdit [17] fine-tunes it to fit the specific target video.

One related reference-based video processing task is video colorization [42, 43]. The colored image retains the exact same grayscale as the uncolored version. It cannot transfer a light color to a dark region within a grayscale image, nor change the texture or style for general editing tasks (as illustrated in Figure 7).

**Spatial-Aligned Conditional Generative Model.** Spatial-aligned conditional generation [23, 28, 45] has been extensively studied in the context of diffusion models. Notable methods include ControlNet [45], which introduces a residual branch to process the conditional image and applies spatially-aligned additions to the main branch. Data collection involves collecting large amounts of images and applies the corresponding image processing techniques (e.g., Canny edge detection or depth estimation) to generate conditions, forming training pairs. This can be regarded as obtaining shared-pattern degradation. Various common types of known degradation, such as Gaussian Blur [14], Tile [19], and grayscale [18], have corresponding ControlNet. In our problem setting, correspondence as CiA guidance can be regarded as a compounded degradation. Recently, DiT-based diffusion models [3, 5, 26] have demonstrated significant advantages over U-Net models in terms of imaging quality and prompt understanding. Many works [31, 32, 47] fine-tuning these base model for conditional generation, demonstrating faster convergence and reduced training data requirements compared to ControlNet.

### 3. Method

Given a set of consistent sequences of images from a specific video, we select one anchor frame  $I^{\text{anc}}$  and edit it exclusively at the appearance level (ensuring spatial alignment, e.g., using ComfyUI with Canny ControlNet) to obtain the reference frame  $I^{\text{ref}}$ . For each target frame  $I^{\text{tgt}}$  of the output video, we compose a triplet:  $(I^{\text{anc}}, I^{\text{ref}}, I^{\text{tgt}})$ . Our goal is to generate the output image frame  $I^{\text{out}}$ , which depicts the structure present in  $I^{\text{tgt}}$  while incorporating the appearance edited in  $I^{\text{ref}}$ . The frame  $I^{\text{anc}}$  serves as a connection since  $I^{\text{anc}}$  and  $I^{\text{ref}}$  are spatially aligned, and

the matching between  $I^{\text{anc}}$  and  $I^{\text{tgt}}$  is termed correspondence [20, 33, 44]. In our work, we utilize a pre-trained Stable Diffusion model [29], with VAE encoding the image  $I$  into the latent representation  $z_0$ , and DDIM inversion [30] to obtain the noisy latent  $z_t$ . During inversion, attention features in the intermediate steps are preserved. Similar to previous works [2, 6], our method produces an image from a denoising process starting from  $z_t^{\text{tgt}}$ , with feature injections from the reference image. This process is referred to as Cross-image Attention, which is an extension of Self-Attention. We first review these two mechanisms.

#### 3.1. Preliminaries

**Self-Attention (SA) and Cross-image Attention (CiA).** Self-Attention (SA) serves as a fundamental component in diffusion models for establishing the global structure. Given an input latent  $z_t$  comprising  $h \times w$  tokens, the intermediate feature in the U-Net  $\phi(z_t)$  employs SA linear projections  $\ell_q, \ell_k$ , and  $\ell_v$ , which map the input image features  $z_t$  onto the query, key, and value matrices of a specified dimension  $d$ :  $Q = \ell_q(\phi(z_t))$ ,  $K = \ell_k(\phi(z_t))$ ,  $V = \ell_v(\phi(z_t))$ , respectively. The attention map  $Attn$  is defined as:  $Attn = \text{Softmax}\left(\frac{Q \cdot K^T}{\sqrt{d}}\right)$ , which computes the similarity among the tokens. The output is defined as the aggregated feature of  $V$  weighted by similarity, denoted as  $\phi(z_t) = Attn \cdot V$ .  $Attn$  can represent the structure of a target image when applying DDIM inversion [30], while  $V$  contains appearance information. During inversion, intermediate  $Q^{\text{tgt}}, K^{\text{tgt}}, V^{\text{tgt}}$  are saved and selected for injection into the denoising process for different tasks, e.g., editing [11, 36], style transfer [6, 39].

Cross-image Attention (CiA) extends the concept of Self-Attention (SA) to multiple images. When  $Q$  is derived from the target image, and  $K$  and  $V$  come from a reference image, CiA measures the similarity between tokens from the target (tgt) and reference (ref) images:  $Attn = \text{Softmax}\left(\frac{Q^{\text{tgt}} \cdot K^{\text{ref}T}}{\sqrt{d}}\right)$ . This similarity weights the reference  $V^{\text{ref}}$  to transfer information to the target output:  $Attn \cdot V^{\text{ref}}$ , which is used in style transfer tasks [6].  $K^{\text{ref}}$  and  $V^{\text{ref}}$  can be extended to multiple images, which is beneficial in video processing tasks [27, 40]. Although CiA represents similarity and is useful for style transfer, it does not ensure accurate correspondence between  $I^{\text{ref}}$  and  $I^{\text{tgt}}$ . The distribution of CiA is scattered, implying that a token in  $I^{\text{tgt}}$  may interact with numerous tokens in  $I^{\text{ref}}$ . This interaction averages their  $V^{\text{ref}}$ , including irrelevant ones, and ultimately leads to the color leakage problem (as shown in the last column of Figure 3). Some works introduce a temperature  $\tau$  to enhance the contrast of attention maps, encouraging focus on a few patches [6]. Others boost contrast by increasing the variance of the attention maps [2]. However, CiA still struggles to establish correspondence for spatially unaligned samples



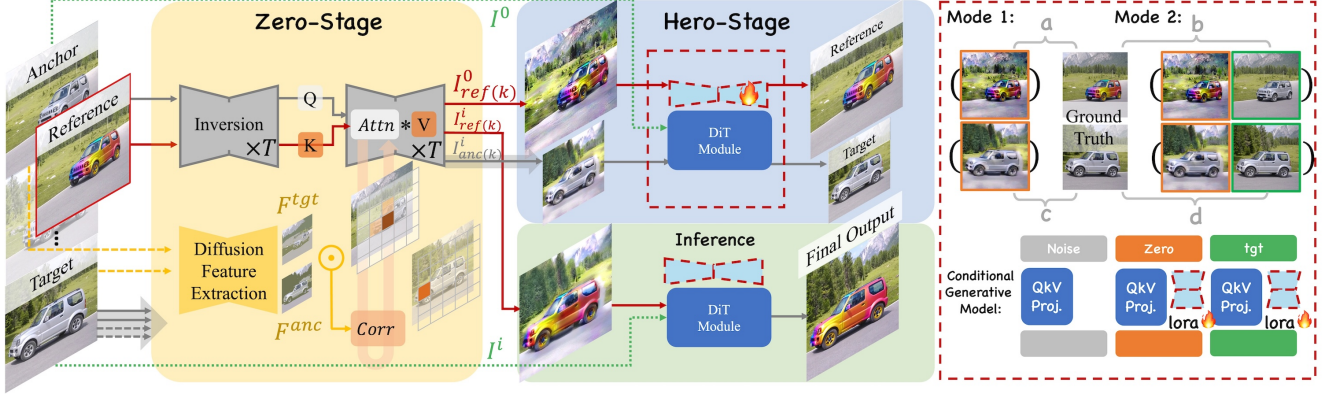


Figure 2. Our framework. **Zero-Stage:** Correspondences ( $Corr$ ) estimated from the anchor and target frames are utilized to guide Cross-image Attention ( $Attn$ ) between the reference and anchor frames, enabling accurate appearance transfer in a zero-shot manner. **Hero-Stage:** We learn a conditional generative model by incorporating LoRA to process conditional tokens. There are two modes of condition injection: one condition with one LoRA (Mode 1) and two conditions with two independent LoRAs (Mode 2). Four pairs of images serve as potential training data, from a to d (see Table 1).

in videos with significant motion, making accurate appearance transfer a research challenge.

**Correspondence from Diffusion Features.** Diffusion models exhibit strong semantic feature extraction capabilities [20, 33, 44]. These studies investigate which intermediate Diffusion Features (DIFT) are the most effective for establishing semantic correspondence. They add noise at a specific timestep  $t$  and feed the noisy latent into the U-Net. Intermediate features from the decoder are extracted through a single denoising step. In our work, we denote intermediate features as  $F$ . Similarly to  $Attn$  in CiA, the semantic correspondence is based on dot product similarity:  $Corr = F^{tgt} \cdot F^{ancT}$ . The correspondence between  $F^{tgt}$  and  $F^{anc}$  is more accurate than that between  $F^{tgt}$  and  $F^{ref}$ , as both are derived from the original video. Since  $F^{anc}$  and  $F^{ref}$  are spatially aligned,  $Corr$  can be used to guide CiA between  $F^{tgt}$  and  $F^{ref}$ .

Previous works have exploited this correspondence for one-to-one pixel-level swapping [44]. The output often contains noticeable pixel boundaries and artifacts caused by inaccurate matching. A recent study [37] adapts a sliding-window-based strategy based on the target video. However, as a text-guided method, it heavily relies on DDIM inversion of the original frames and text prompts, without explicitly incorporating  $V$  from the reference. This significantly limits its ability to perform free editing with complex appearance changes. Additionally, it requires many hyper-parameters for each case, such as the number of steps for DDIM feature injection and the size of the sliding window. This is an inherent drawback of training-free methods.

### 3.2. Zero-Stage: Correspondence as CiA Guidance

We propose using correspondence as accurate guidance for CiA  $Attn$ , through the implementation of masked atten-

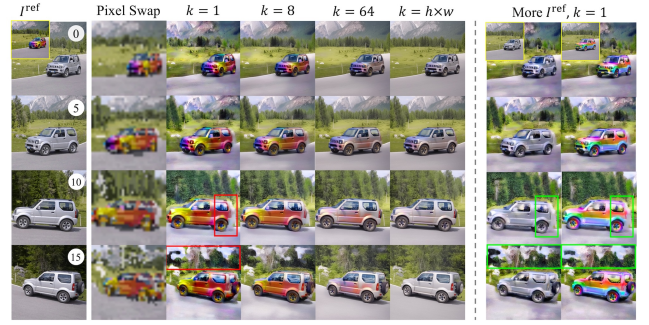


Figure 3. **Left:**  $Corr$  guidance with increasing  $k$ . When  $k = h \times w$ , it corresponds to the original Cross-image Attention. **Right:** Using other references results in similar missing patterns (red and green boxes).

tion. The mask is created by selecting the top- $k$  entries in  $Corr$  and setting these positions to 1 in the mask matrix  $M(Corr, k)$ , where  $k$  ranges from 1 to the total number of tokens  $h \times w$ . These selected places are assigned a large value in the original attention score matrix  $A$ , resulting in  $A \oplus M(Corr, k)$ , before the softmax operation. Using this guided attention and  $V^{ref}$  from the reference, a denoising step is:

$$\hat{z}_{t-1}^{tgt} = \epsilon_{\theta}(z_t^{tgt}, A \oplus M(Corr, k), V^{ref}) \quad (1)$$

where  $\hat{z}_{t-1}^{tgt}$  will be iteratively denoised until obtaining the clean latent  $\hat{z}_0^{tgt}$ , thereby achieving appearance transfer. The final transferred result of the target frame  $I^{tgt}$  is termed as  $I_{M(k)}^{tgt}$ .

The selection of  $k$  is challenging. As shown in Figure 3, we apply different  $k$  values on four frames, including anchor frame 0. When  $k = 1$ , the accurate semantic cor-



responsiveness can successfully transfer each part of the car to the target image with corresponding colors. However, the modifications applied to the original attention mechanism are substantial, leading to compounded degradation in imaging quality, including irregular blurring and color over-saturation. The former is caused by the collapsed structure within the attention map, while the latter arises from the increased feature magnitude due to the low entropy of the identity matrix [16]. As  $k$  increases, the imaging quality gradually returns to normal, while the influence of *Corr* guidance decreases. When  $k = h \times w$ , it is equivalent to the original CiA, facing the same problems of color leakage and inaccurate appearance transfer.

Based on the above analysis, it is difficult to find an appropriate  $k$  that achieves a satisfying result across the whole image in zero-shot manner. Intuitively, imaging degradation is less harmful than color leakage and offers greater potential for post-processing. We observed that, for different frames, the degradation pattern is similar. We also have the ground-truth high-quality version of  $I_{M(k)}^{\text{anc}}$ , which is  $I^{\text{ref}}$ . Therefore, a natural question arises: *can we train a conditional generative model to restore images with compounded degradation caused by masked attention?*

### 3.3. Hero-Stage: Zero-Stage as Condition

We use the intermediate result from the Zero-Stage as the image condition and perform Holistic vidEo RestOration, with irregular blurring and color over-saturation issues. When training on the pair  $\{I_{M(k)}^{\text{anc}}, I^{\text{ref}}\}$ , it certainly guarantees fitting on this anchor frame. We investigate its ability to generalize to subsequent frames, particularly long-range frames with substantial motion.

#### 3.3.1 Generalization Across Video

For target frames that are near the anchor frame (e.g., frame 5 in Figure 3), the color over-saturation and blurring patterns are similar to the anchor frame. However, for long-range target frames (frames 10 and 15), in addition to the two aforementioned aspects of degradation, there is also a noticeable color-missing issue caused by unsuccessful matching in significantly changed backgrounds (highlighted in the red box). This color-missing issue does not occur in the training anchor frame pair, so the trained model is more likely to preserve these missing parts instead of restoring them. Extracting masks for unchanged regions and straightforward replacement of the original target can be sensitive to mask extraction errors. These methods may also fail due to the lack of clear segmentation between objects and the background. To address this, we aim to incorporate the target frames into the training pipeline, automatically providing auxiliary information. There are two potential ways to use target frames  $I^{\text{tgt}}$ :

a. zero-ref	$\{I_{\text{ref}(k)}^0, I^{\text{ref}}\}$	Mode 1
b. (zero, tgt)-ref	$\{(I_{\text{ref}(k)}^0, I^0), I^{\text{ref}}\}$	Mode 2
c. zero-tgt	$\{I_{\text{anc}(k)}^i, I^i\}$	Mode 1
d. (zero, tgt)-tgt	$\{(I_{\text{anc}(k)}^i, I^i), I^i\}$	-

Table 1. Pairs of training data. Mode 1 use a and c, Mode 2 use b. d may cause the model to overfit on the target  $I^i$  due to the shortcut.

**Mode 1: Implicit Usage.** We encourage the model to implicitly learn unseen regions through the provision of auxiliary training pairs. We use  $I^{\text{anc}}$  as the reference to construct a series of frames  $\{I_{\text{anc}(k)}^0, \dots, I_{\text{anc}(k)}^n\}$ . As shown in Figure 3 on the right, frames 10 and 15, with other references, display similar missing regions (in the green box) as when  $I^{\text{ref}}$  is used as the reference. Specifically, when using  $I^{\text{anc}}$  as the reference, the corresponding ground truth for each target frame should be to reconstruct themselves. These auxiliary training pairs are termed zero-tgt:  $\{I_{\text{anc}(k)}^i, I^i\}, i = [0, n]$ .

**Mode 2: Explicit Usage.** We can also explicitly use original target frames by introducing an additional conditional branch, denoted as  $\{(I_{\text{ref}(k)}^0, I^0), I^{\text{ref}}\}$ . Ideally,  $I_{\text{ref}(k)}^0$  provides an appearance-transferred intermediate result, while  $I^0$  provides a shortcut to quickly reconstruct the unchanged region. This training pair is termed (zero, tgt)-ref. Similarly, we can construct (zero, tgt)-tgt pairs:  $\{(I_{\text{anc}(k)}^i, I^i), I^i\}$ .

In summary, all potential training pairs are shown in Table 1. Mode 1 contains a + c, and Mode 2 contains b + d. Regardless of the usage, fitting the anchor frame can always be guaranteed. The key challenge lies in ensuring that the target frame provides only auxiliary information of the unchanged region while preventing the leakage of its appearance.

#### 3.3.2 Explicit Condition Avoids Leakage

As shown in Figure 4, Mode 1 with a + c achieves better preservation of the outline of the car compared to only a, although the missing regions in the background remain unreparable. In Mode 2, with the explicit injection of the target frame, the background can be successfully repaired. This suggests that the explicit mode can differentiate between edited and non-edited regions: for the edited object regions, it restores the Zero-Stage intermediate results, while for unchanged regions, it directly uses a shortcut to copy from the target frame.

When the editing type involves texture or style rather than only color change (second row, reference is watercolor style), Mode 1 with training pair c forces the model to learn zero-tgt on each target frame, causing the model to overfit them. As a result, the style is not successfully changed, and the color layout from the Zero-Stage is not used (zoom in on the red box). Conversely, Mode 2 explicit injection

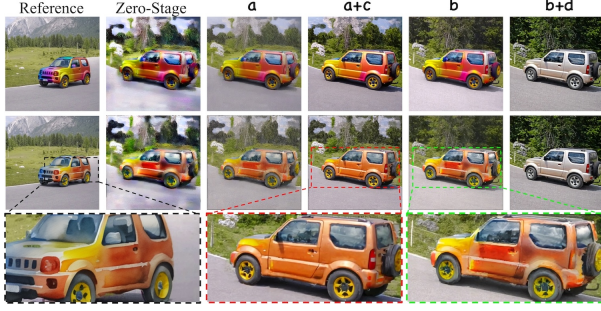


Figure 4. Mode 1 (a+c) can better preserve target structure of car than only using a, but it struggles with style transfer (e.g., watercolor in the second row) and restoring severely missing background regions. Mode 2 (b) can solve two problems. d will result in appearance leakage of target frame.

appears likely to leak the appearance of the target image, but it does not. This indicates that the training of the two conditional branches does not cause conflicts, and they can clearly differentiate their respective roles. The appearance of the subsequent frames is successfully transferred to the watercolor style (zoom in on the green box). For data pair d,  $\{(I_{\text{anc}(k)}^i, I^i), I^i\}$ , the model identifies shortcuts from the second condition to the target frame  $I^i$ . Even if the first condition is changed to  $\{I_{\text{ref}(k)}^i\}$ , the output still directly corresponds to the second condition. Therefore, it should not be involved in training.

### 3.3.3 Balancing Condition Branches

Since we have the Hero-Stage, can we use less-than-perfect intermediate results in the Zero-Stage, such as performing direct pixel swapping without introducing a generative process, to save time? As shown in Figure 3, pixel swapping according to correspondence can also provide an initialization of the transferred result, although it contains less information or might be inaccurate. Can it achieve the same level of conditional control as our Zero-Stage initialization?

We emphasize the importance of *condition balance*, i.e., two branches should ideally contain equal amounts of information. Otherwise, the model will be overly reliant on the side that provides more information. Since pixel swapping does not provide enough structural information but only the color layout, it will force the model to rely too much on the second condition, the target frame, to acquire structure and details of texture for the reconstruction of the reference. When the target frame has a totally different texture or style compared to the reference, the model will be confused about condition usage. In the most likely scenario, this degenerates into a recolor task, i.e., using pixel swapping to recolor the target image.

For the implementation of conditional generative mod-

els, in the past UNet-diffusion era, it was always implemented by ControlNet [45], with high computational cost and slow convergence. In our task, we only need to focus on a set of images from one video, and the conditional degraded image itself contains sufficient appearance information, which is much simpler than training a general conditional model like canny or depth. Recently, with the development of DiT-based diffusion models, injection paradigms have largely changed. These methods [31, 47] typically convert conditional images into image token sequences, concatenate them with noise latent representations, and fine-tune DiT modules with LoRA to process conditional tokens. The conditional tokens share the same positional encoding as the corresponding spatially-aligned noisy tokens, which accelerates convergence. With this efficient fine-tuning architecture and our solid Zero-Stage initialization, our Hero-Stage achieves faster convergence. For mode 2, two independent LoRAs are necessary for model to distinguish different control purpose.

## 4. Experiments

### 4.1. Experimental Settings

#### 4.1.1 Datasets

We utilize datasets from two sources. We use a collection of videos utilized in video editing baselines [41]. These videos have all been uniformly sampled to 16 frames. For each video, we experiment on two sub-tasks. The first sub-task is Colorization, where we convert the target video to grayscale, and the reference is the original anchor frame. The second sub-task is general appearance editing (General-Edit), where the references are processed using Stable Diffusion WebUI with multiple ControlNets for spatial alignment. The editing types include color changes (*a car in the color red, blue, etc.*), texture changes (*a car made of clay*), and style changes (*a car in watercolor style*). The colorization task supports deterministic evaluation metrics including PSNR, LPIPS, and SSIM for each frame. For General-Edit, there is no ground truth available except for the anchor frame. Therefore, we employ auxiliary metrics to evaluate temporal consistency, including Motion Smoothness (MS) and Subject Consistency (SC), as proposed in VBench [12]. The colorization task does not cover the general appearance editing task, and General-Edit lacks ground truth, making the evaluation indirect. To address this, we construct a dataset using Blender. We collect five 3D objects, each prepared with two distinct appearances. We employ two classic camera movements: panning and zooming in. The dataset, Blender-Color-Edit, is illustrated in Figure 5.

	Colorization			Blender-Color-Edit			General-Edit				
Method	PSNR ( $\uparrow$ )	LPIPS ( $\downarrow$ )	SSIM ( $\uparrow$ )	PSNR ( $\uparrow$ )	LPIPS ( $\downarrow$ )	SSIM ( $\uparrow$ )	MS ( $\uparrow$ )	SC ( $\uparrow$ )	PSNR $_{\dagger}$ ( $\uparrow$ )	LPIPS $_{\dagger}$ ( $\downarrow$ )	SSIM $_{\dagger}$ ( $\uparrow$ )
AnyV2V	22.7450	0.1456	0.7703	23.3208	0.1316	0.8174	0.9192	0.8325	26.2379	0.0935	0.8392
I2VEdit	23.4085	0.1231	0.8219	24.1103	0.1317	0.8044	0.9329	0.8724	<b>27.0925</b>	<u>0.0830</u>	<u>0.8639</u>
CiA ( $\beta^*$ )	23.2932	0.1486	0.7975	23.0619	0.1377	0.7686	<u>0.9409</u>	<b>0.9158</b>	25.5291	0.0943	0.8239
Ours	<b>28.2063</b>	<b>0.0491</b>	<b>0.9298</b>	<b>26.7640</b>	<b>0.0565</b>	<b>0.8546</b>	<b>0.9428</b>	<u>0.8978</u>	<u>26.7768</u>	<b>0.0558</b>	<b>0.8886</b>

Table 2. Results on three appearance editing tasks for all reference-guided methods. For Colorization and Blender-Color-Edit, all frames have ground truth to calculate PSNR (dB), LPIPS, and SSIM. For General-Edit, calculations can only be performed on the anchor frame ( $\dagger$ ) using the reference as ground truth. Motion Smoothness (MS) and Subject Consistency (SC) are utilized to evaluate temporal consistency.



Figure 5. Blender-Color-Edit dataset, rendered in Blender.

#### 4.1.2 Baselines

We compare our approach with two reference-based video editing methods, namely AnyV2V [15] and I2VEdit [24], along with an appearance transfer method, CiA with attention contrast [2] employing Stable Diffusion. AnyV2V directly utilizes I2VGen-XL, applying DDIM Inversion and selectively injecting features during the denoising process. It requires varying hyperparameters for each scenario, including the injection rate at spatial, temporal, and feedforward modules. Following its setting, we adopt an inversion step of 500 and a denoising step of 50, traversing the rates across  $[0.2, 0.5, 0.8]$ , and selecting the optimal result for each scenario. I2VEdit initially performs LoRA fine-tuning of the temporal module of SVD to adapt to the motion pattern of the target video. We follow its setting by adopting a LoRA rank of  $r = 32$ . For optimization steps, we employ sufficient steps of  $t = 1000$ , selecting the best results that balance the fidelity of the motion pattern and reference. The appearance transfer method [2] employs Cross-image Attention (CiA) for semantic matching between two images. It applies a contrast value  $\beta$  to the attention map for more accurate transfer, alongside a guidance value  $\alpha$  to diverge from the original appearance. We follow the setting with  $\alpha = 3.5$ . We observed that the original setting  $\beta = 1.67$  may introduce significant structural changes. Thus, we traverse  $\beta$  across  $[1, 1.33, 1.67]$  and select the best, referred to as CiA ( $\beta^*$ ). For our method, we set  $k = 1$  at Zero-Stage for all experiments as the default choice. We perform

fine-tuning at a resolution of 512 and an optimization step  $t = 400$  by default, utilizing the default LoRA configuration from EasyControl [47], with  $r = 128$ ,  $\alpha = 128$ .

## 4.2. Comparison with Baselines

### 4.2.1 Qualitative Results

Figure 6 showcases a challenging scenario characterized by substantial object motion, dynamic background changes, and a complex color layout in the reference. AnyV2V shows considerable degradation in imaging quality when tackling such complex motion. I2VEdit adequately fits the motion within 600 steps for this case; however, at this point, the appearance of the reference can no longer effectively control the subsequent frames. This suggests that for videos with complex motion significantly deviating from the pre-trained I2V domain, achieving a balance between motion fitting and reference control in I2V is challenging. The basic CiA method, which applies an optical contrast  $\beta^*$  to attention maps for accurate transfer, alters the structure of the target frame. While this may be acceptable for appearance transfer tasks involving two different objects without a need for strict structure preservation, it is unsuitable for video editing, where maintaining structural consistency of the target frame is crucial. Furthermore, without incorporating more accurate correspondence mechanisms such as DIFT, there can be inaccurate matches leading to missing color on the car’s body. Our Zero-Stage approach, augmented with DIFT correspondence guidance, ensures structure preservation and consistent appearance transfer of the car, while the Hero-Stage can further mitigate degradation.

Figure 7 left show results in Blender-Color-Edit dataset. With their simpler motion, I2VEdit can strike a balance between motion fitting and reference control, achieving visually acceptable results at an intuitive level. However, imaging quality degradation still occurs (zoom in on the red box).

We also compare our method with recent commercial services, Kling<sup>1</sup>, with its online service of reference-based video editing. It supports mask tracking, which requires the user to click and select the region of the object to be edited and track it throughout the video. As shown in Fig-

<sup>1</sup><https://app.klingai.com/global/>



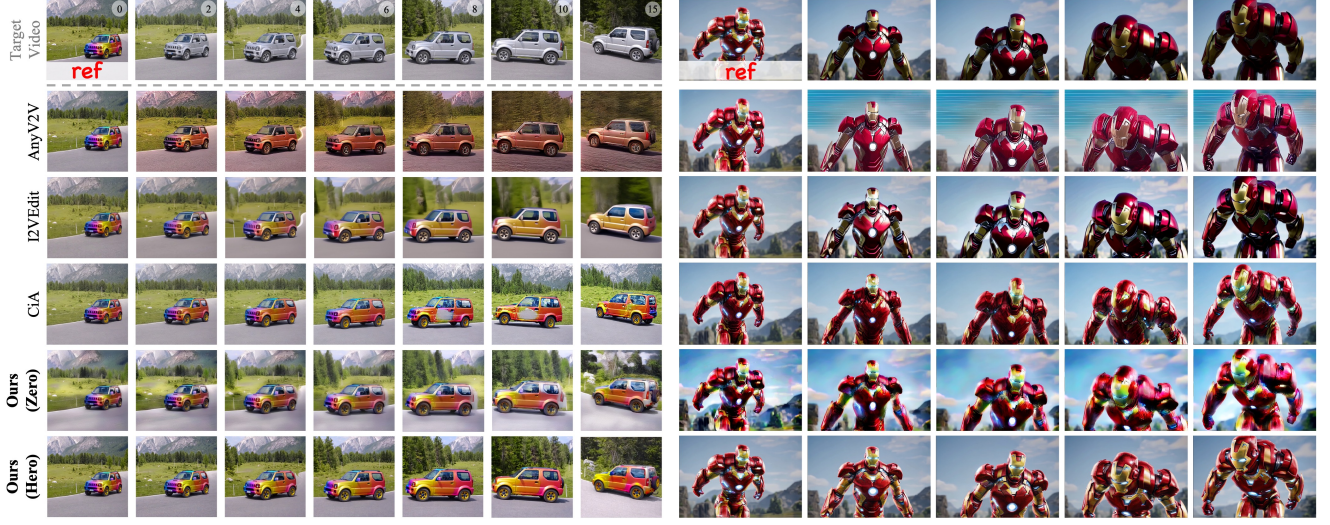


Figure 6. Qualitative results on General-Edit dataset. Our method maintains the highest consistent fidelity to reference appearance and target video structure.

ure 8, the commercial models, with their superior temporal modeling, achieve better appearance consistency compared to I2VEdit with open-source lightweight I2V model. However, in terms of appearance details, it still falls short of what our method can achieve. Additionally, their motion fidelity to the target video is not guaranteed, and the imaging quality also deteriorates.

#### 4.2.2 Quantitative Results

In Table 2, we evaluate the methods quantitatively across three sub-tasks. For the General-Edit task, our method demonstrates superior performance in Motion Smoothness. CiA, with the optimally-searched attention contrast  $\beta^*$ , exhibits the highest Subject Consistency, but sacrifices the preservation of the target structure, resulting in the lowest PSNR on the anchor frame. As illustrated in Figure 6, with a changing background, it consistently utilizes the background from the reference frame rather than preserving the original background. This leads to the highest Subject Consistency score, yet obscures issues of appearance inconsistency and structural deformation of the car. Multiple indirect metrics need to be evaluated concurrently. Our method attains the best or second-best performance across all metrics. For the Colorization and Blender-Color-Edit tasks, which allow for strict evaluation with ground truth, our method clearly achieves the highest scores.

### 4.3. Ablation Studies

#### 4.3.1 Combinations of Training Data Pairs

We have four paired datasets, as presented in Table 1. We also investigate the feasibility of directly learning the trans-

	$t = 600$ (400 for Mode 2)			$t = 1000$		
	avg	anc	tgt( $\Delta$ )	avg	anc	tgt( $\Delta$ )
tgt-ref	19.38	22.29	17.52 <sub>(-4.77)</sub>	22.39	27.09	18.62 <sub>(-8.47)</sub>
zero-ref	24.09	29.57	20.95 <sub>(-8.62)</sub>	24.59	31.80	20.92 <sub>(-10.88)</sub>
Mode 1	24.54	28.79	22.08 <sub>(-6.71)</sub>	25.77	30.92	22.91 <sub>(-8.01)</sub>
Mode 2	<b>26.76</b>	28.91	25.51 <sub>(-3.40)</sub>	<b>27.38</b>	29.97	25.65 <sub>(-4.32)</sub>

Table 3. Ablation of training pairs on Blender-Color-Edit dataset: PSNR( $\uparrow$ ) of avg: average across all frames; anc: anchor frame; tgt: last target frame;  $\Delta$  represents difference between tgt and anc. For 1 condition (tgt-ref, zero-ref, Mode 1), we evaluate at  $t = 600$ , for 2 conditions (Mode 2), we evaluate at  $t = 400$ , to ensure the same optimization time consumption.

fer from an anchor frame to a reference frame and generalizing this to subsequent target frames, referred to as tgt-ref. We conduct ablation studies using our constructed Blender-Color-Edit dataset to better discern the performance of each method. For each scenario, we perform training three times and compute the average to mitigate the effects of randomness in LoRA fine-tuning.

As shown in Table 3, when directly fine-tuning the model to transfer the original anchor frame to the reference (tgt-ref) with sufficient  $t = 1000$  optimization steps, although the PSNR on the anchor frame reaches 27.09, the last target frame remains at 18.62, indicating a complete lack of generalization. As shown on the left side of Figure 7, the anchor frame in the first row fits perfectly; however, in the subsequent frames (rows 2 and 3), there is noticeable leakage of the target appearance.

With Zero-Stage as initialization, zero-ref achieves a higher PSNR across all target frames on average. However,

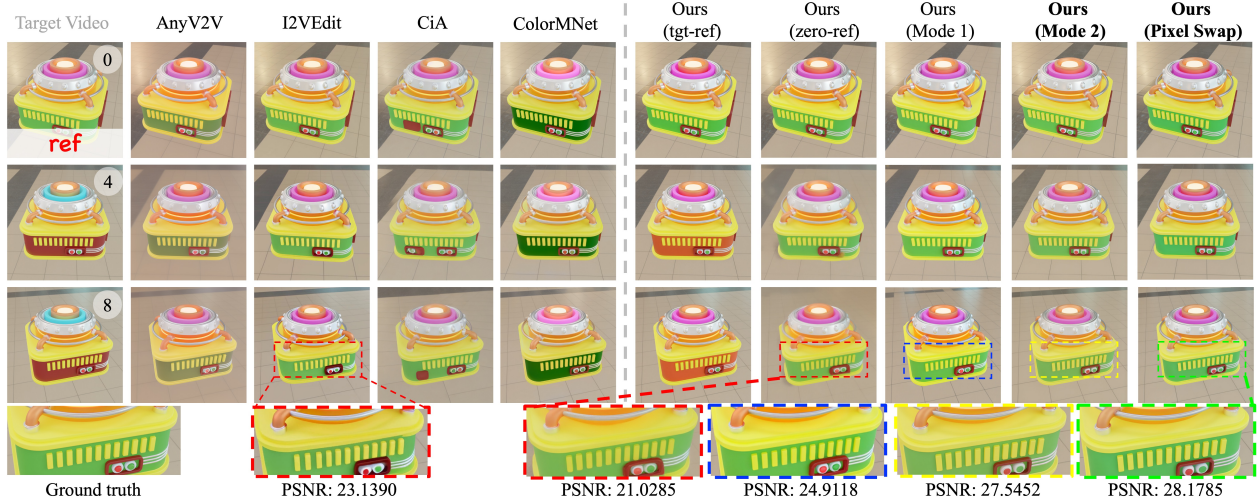


Figure 7. Qualitative results on Blender-Color-Edit dataset. **Left**: comparison with baselines. ColorMNet is proposed for colorization task. We convert target frames into grayscale for comparison, while it cannot transfer light green to dark region. **Right**: Ablations on training pairs. Mode 2 with Zero-Stage or Pixel Swap initialization achieve higher PSNR than other pairs.

the generalization ability is limited; even with more optimization steps, the gap between the anchor frame and the last target frame remains substantial ( $\Delta = -10.88$ ). We then further introduce an auxiliary target frame. With Mode 1, this gap is reduced to 8.01. With Mode 2, the gap is further narrowed to 4.32, reaching the highest average PSNR of 27.38. Moreover, Mode 2 demonstrates notably faster convergence. Mode 2 with two conditions consumes 1.5 times the training time per step compared to the others with one condition. For fair comparison, we evaluate Mode 2 at  $t = 400$  while the others at  $t = 600$ . Under the same optimization time, Mode 2 achieves the highest average PSNR and the smallest gap between the anchor frame and the last target frame.

### 4.3.2 Zero-Stage Initialization

We emphasize the importance of Zero-Stage initialization. As illustrated in Table 4, during the early optimization steps at  $t = 200$ , our Zero-Stage initialization shows a faster increase in PSNR compared to pixel swap initialization and stabilizes at a slightly higher average PSNR by  $t = 400$ . There is no obvious advantage visible at the visual level. Especially, when we analysis each case, we find some cases, pixel swap initialization achieve a higher PSNR score (Figure 7, last two columns). This is because, in the Blender-Color-Edit task, the color transformation involves a complete replacement of colors rather than complex color editing. Even with a pixel swap color layout lacking sufficient details, the model is still capable of blending the color layout into the target frame effectively.

For the General-Edit task with more complicated edit-

Setting	$t = 200$	$t = 400$
Pixel Swap	22.4982	26.1908
Zero-Stage Initialization	<b>23.7836</b>	<b>26.7640</b>

Table 4. Ablation on Zero-Stage initialization on Blender-Color-Edit dataset, which leads to a faster convergence in Hero-Stage and stabilize at a higher PSNR.

ing, the advantage of Zero-Stage initialization is more pronounced. As shown in Figure 8, pixel swap initialization fails to provide sufficient appearance information on details (zoom in on the green and yellow box) as our Zero-Stage initialization. Also, in cases involving texture or style changes, pixel swap causes the fine-tuned model to overly depend on the target condition. As a result, it struggles to transfer the reference texture or style to subsequent frames.

## 5. Conclusion

In this paper, we introduce *Zero-to-Hero* for reference-based video appearance editing. By leveraging accurate correspondence to guide Cross-image Attention between reference and target frames, our Zero-Stage ensures fine-grained appearance transfer for videos with large motion. To address the compounded degradation caused by attention intervention, our Hero-Stage learns a conditional generative model based on training pairs from the anchor frame. This approach generalizes effectively across videos and ensures consistent, holistic restoration of the entire video. Experimental results demonstrate the effectiveness of our method, outperforming baselines in terms of high reference fidelity and video temporal consistency.





Figure 8. Qualitative results on General-Edit dataset. **Left:** Pixel swap initialization fails to provide sufficient information, resulting in some detailed appearances in the reference being missed in the subsequent frames (zoomed-in green and yellow box). **Middle/Right:** Pixel swap causes the fine-tuned model to become overly reliant on the target condition, hindering its ability to transfer the reference texture or style to subsequent frames. Kling online service of reference-based editing cannot strictly preserve target video motion (red box).

## Acknowledgment

This work is supported by Key Scientific Research Base for Digital Conservation of Cave Temples (Zhejiang University), State Administration for Cultural Heritage, and Alibaba Research Intern Program. Work done during T. Su’s internship at Alibaba Cloud Computing. Correspondence to: C. Wang and D. Lu.

## References

- [1] Donghoon Ahn, Hyounghwon Cho, Jaewon Min, Wooseok Jang, Jungwoo Kim, SeonHwa Kim, Hyun Hee Park, Kyong Hwan Jin, and Seungryong Kim. Self-rectifying diffusion sampling with perturbed-attention guidance. In *European Conference on Computer Vision*, pages 1–17. Springer, 2024. 2
- [2] Yuval Alaluf, Daniel Garibi, Or Patashnik, Hadar Averbuch-Elor, and Daniel Cohen-Or. Cross-image attention for zero-shot appearance transfer. In *ACM SIGGRAPH 2024 Conference Papers*, pages 1–12, 2024. 2, 3, 7
- [3] black-forest labs. Flux. [Online] <https://github.com/black-forest-labs/flux>, 2023. 3
- [4] Andreas Blattmann, Tim Dockhorn, Sumith Kulal, Daniel Mendelevitch, Maciej Kilian, Dominik Lorenz, Yam Levi, Zion English, Vikram Voleti, Adam Letts, et al. Stable video diffusion: Scaling latent video diffusion models to large datasets. *arXiv preprint arXiv:2311.15127*, 2023. 2
- [5] Junsong Chen, Jincheng Yu, Chongjian Ge, Lewei Yao, Enze Xie, Yue Wu, Zhongdao Wang, James Kwok, Ping Luo, Huchuan Lu, et al. Pixart-alpha: Fast training of diffusion transformer for photorealistic text-to-image synthesis. *arXiv preprint arXiv:2310.00426*, 2023. 3
- [6] Jiwoo Chung, Sangeek Hyun, and Jae-Pil Heo. Style injection in diffusion: A training-free approach for adapting large-scale diffusion models for style transfer. In *Proceedings of the IEEE/CVF Conference on Computer Vision and Pattern Recognition*, pages 8795–8805, 2024. 2, 3
- [7] Yuren Cong, Mengmeng Xu, Christian Simon, Shoufa Chen, Jiawei Ren, Yanping Xie, Juan-Manuel Perez-Rua, Bodo Rosenhahn, Tao Xiang, and Sen He. Flatten: optical flow-guided attention for consistent text-to-video editing. *arXiv preprint arXiv:2310.05922*, 2023. 2
- [8] Dave Epstein, Allan Jabri, Ben Poole, Alexei Efros, and Aleksander Holynski. Diffusion self-guidance for controllable image generation. *Advances in Neural Information Processing Systems*, 36:16222–16239, 2023. 2
- [9] Ruoyu Feng, Wenming Weng, Yanhui Wang, Yuhui Yuan, Jianmin Bao, Chong Luo, Zhibo Chen, and Baining Guo. Ccredit: Creative and controllable video editing via diffusion models. In *Proceedings of the IEEE/CVF Conference on Computer Vision and Pattern Recognition*, pages 6712–6722, 2024. 2
- [10] Michal Geyer, Omer Bar-Tal, Shai Bagon, and Tali Dekel. Tokenflow: Consistent diffusion fea-



- tures for consistent video editing. *arXiv preprint arXiv:2307.10373*, 2023. 2
- [11] Amir Hertz, Ron Mokady, Jay Tenenbaum, Kfir Aberman, Yael Pritch, and Daniel Cohen-Or. Prompt-to-prompt image editing with cross attention control. *arXiv preprint arXiv:2208.01626*, 2022. 3
- [12] Ziqi Huang, Yinan He, Jiashuo Yu, Fan Zhang, Chenyang Si, Yuming Jiang, Yuanhan Zhang, Tianxing Wu, Qingyang Jin, Nattapol Chanpaisit, et al. Vbench: Comprehensive benchmark suite for video generative models. In *Proceedings of the IEEE/CVF Conference on Computer Vision and Pattern Recognition*, pages 21807–21818, 2024. 2, 6
- [13] Ozgur Kara, Bariscan Kurtkaya, Hidir Yesiltepe, James M Rehg, and Pinar Yanardag. Rave: Randomized noise shuffling for fast and consistent video editing with diffusion models. In *Proceedings of the IEEE/CVF Conference on Computer Vision and Pattern Recognition*, pages 6507–6516, 2024. 2
- [14] kohya ss. Gaussian deblur controlnet. [Online] <https://huggingface.co/kohya-ss/controlnet-1llite>, 2023. 3
- [15] Max Ku, Cong Wei, Weiming Ren, Huan Yang, and Wenhui Chen. Anyv2v: A plug-and-play framework for any video-to-video editing tasks. *arXiv preprint arXiv:2403.14468*, 2024. 2, 3, 7
- [16] Bingyan Liu, Chengyu Wang, Tongtong Su, Huan Ten, Jun Huang, Kailing Guo, and Kui Jia. Understanding attention mechanism in video diffusion models. *arXiv preprint arXiv:2504.12027*, 2025. 2, 5
- [17] Chang Liu, Rui Li, Kaidong Zhang, Yunwei Lan, and Dong Liu. Stablev2v: Stabilizing shape consistency in video-to-video editing. *arXiv preprint arXiv:2411.11045*, 2024. 2, 3
- [18] llyasviel. Colorization controlnet. [Online] [https://huggingface.co/llyasviel/sd\\_control\\_collection/blob/main/ioclab\\_sd15\\_recolor.safetensors](https://huggingface.co/llyasviel/sd_control_collection/blob/main/ioclab_sd15_recolor.safetensors), 2023. 3
- [19] llyasviel. Tile controlnet. [Online] [https://huggingface.co/llyasviel/ControlNet-v1-1/blob/main/control\\_v11fle\\_sd15\\_tile.pth](https://huggingface.co/llyasviel/ControlNet-v1-1/blob/main/control_v11fle_sd15_tile.pth), 2023. 3
- [20] Grace Luo, Lisa Dunlap, Dong Huk Park, Aleksander Holynski, and Trevor Darrell. Diffusion hyperfeatures: Searching through time and space for semantic correspondence. *Advances in Neural Information Processing Systems*, 36, 2024. 2, 3, 4
- [21] Chong Mou, Xintao Wang, Jiechong Song, Ying Shan, and Jian Zhang. Dragondiffusion: Enabling drag-style manipulation on diffusion models. *arXiv preprint arXiv:2307.02421*, 2023. 2
- [22] Chong Mou, Xintao Wang, Jiechong Song, Ying Shan, and Jian Zhang. Diffeditor: Boosting accuracy and flexibility on diffusion-based image editing. In *Proceedings of the IEEE/CVF Conference on Computer Vision and Pattern Recognition*, pages 8488–8497, 2024. 2
- [23] Chong Mou, Xintao Wang, Liangbin Xie, Yanze Wu, Jian Zhang, Zhongang Qi, and Ying Shan. T2i-adapter: Learning adapters to dig out more controllable ability for text-to-image diffusion models. In *Proceedings of the AAAI conference on artificial intelligence*, pages 4296–4304, 2024. 3
- [24] Wenqi Ouyang, Yi Dong, Lei Yang, Jianlou Si, and Xingang Pan. I2vedit: First-frame-guided video editing via image-to-video diffusion models. In *SIGGRAPH Asia 2024 Conference Papers*, pages 1–11, 2024. 2, 3, 7
- [25] Taesung Park, Jun-Yan Zhu, Oliver Wang, Jingwan Lu, Eli Shechtman, Alexei Efros, and Richard Zhang. Swapping autoencoder for deep image manipulation. *Advances in Neural Information Processing Systems*, 33:7198–7211, 2020. 2
- [26] William Peebles and Saining Xie. Scalable diffusion models with transformers. In *Proceedings of the IEEE/CVF international conference on computer vision*, pages 4195–4205, 2023. 3
- [27] Chenyang Qi, Xiaodong Cun, Yong Zhang, Chenyang Lei, Xintao Wang, Ying Shan, and Qifeng Chen. Fatezero: Fusing attentions for zero-shot text-based video editing. In *Proceedings of the IEEE/CVF International Conference on Computer Vision*, pages 15932–15942, 2023. 3
- [28] Can Qin, Shu Zhang, Ning Yu, Yihao Feng, Xinyi Yang, Yingbo Zhou, Huan Wang, Juan Carlos Niebles, Caiming Xiong, Silvio Savarese, et al. Unicontrol: A unified diffusion model for controllable visual generation in the wild. *arXiv preprint arXiv:2305.11147*, 2023. 3
- [29] Robin Rombach, Andreas Blattmann, Dominik Lorenz, Patrick Esser, and Björn Ommer. High-resolution image synthesis with latent diffusion models. In *Proceedings of the IEEE/CVF Conference on Computer Vision and Pattern Recognition*, pages 10684–10695, 2022. 3
- [30] Jiaming Song, Chenlin Meng, and Stefano Ermon. Denoising diffusion implicit models. *arXiv preprint arXiv:2010.02502*, 2020. 3
- [31] Zhenxiong Tan, Songhua Liu, Xingyi Yang, Qiaochu Xue, and Xinchao Wang. Ominicontrol: Minimal and universal control for diffusion transformer. *arXiv preprint arXiv:2411.15098*, 2024. 3, 6
- [32] Zhenxiong Tan, Qiaochu Xue, Xingyi Yang, Songhua Liu, and Xinchao Wang. Ominicontrol2: Effi-

cient conditioning for diffusion transformers. *arXiv preprint arXiv:2503.08280*, 2025. 3

- [33] Luming Tang, Menglin Jia, Qianqian Wang, Cheng Perng Phoo, and Bharath Hariharan. Emergent correspondence from image diffusion. *Advances in Neural Information Processing Systems*, 36: 1363–1389, 2023. 2, 3, 4
- [34] Yoad Tewel, Omri Kaduri, Rinon Gal, Yoni Kasten, Lior Wolf, Gal Chechik, and Yuval Atzmon. Training-free consistent text-to-image generation. *ACM Transactions on Graphics (TOG)*, 43(4):1–18, 2024. 2
- [35] Narek Tumanyan, Omer Bar-Tal, Shai Bagon, and Tali Dekel. Splicing vit features for semantic appearance transfer. In *Proceedings of the IEEE/CVF Conference on Computer Vision and Pattern Recognition*, pages 10748–10757, 2022. 2
- [36] Narek Tumanyan, Michal Geyer, Shai Bagon, and Tali Dekel. Plug-and-play diffusion features for text-driven image-to-image translation. In *Proceedings of the IEEE/CVF Conference on Computer Vision and Pattern Recognition*, pages 1921–1930, 2023. 3
- [37] Jiangshan Wang, Yue Ma, Jiayi Guo, Yicheng Xiao, Gao Huang, and Xiu Li. Cove: Unleashing the diffusion feature correspondence for consistent video editing. *arXiv preprint arXiv:2406.08850*, 2024. 1, 2, 4
- [38] Haofei Xu, Jing Zhang, Jianfei Cai, Hamid Rezaatoughi, and Dacheng Tao. Gmflow: Learning optical flow via global matching. In *Proceedings of the IEEE/CVF conference on computer vision and pattern recognition*, pages 8121–8130, 2022. 2
- [39] Youcan Xu, Zhen Wang, Jun Xiao, Wei Liu, and Long Chen. Freetuner: Any subject in any style with training-free diffusion. *arXiv preprint arXiv:2405.14201*, 2024. 3
- [40] Shuai Yang, Yifan Zhou, Ziwei Liu, and Chen Change Loy. Rerender a video: Zero-shot text-guided video-to-video translation. In *SIGGRAPH Asia 2023 Conference Papers*, pages 1–11, 2023. 1, 2, 3
- [41] Shuai Yang, Yifan Zhou, Ziwei Liu, and Chen Change Loy. Fresco: Spatial-temporal correspondence for zero-shot video translation. In *Proceedings of the IEEE/CVF Conference on Computer Vision and Pattern Recognition*, pages 8703–8712, 2024. 1, 2, 3, 6
- [42] Yixin Yang, Jiangxin Dong, Jinhui Tang, and Jinshan Pan. Colormnet: A memory-based deep spatial-temporal feature propagation network for video colorization. In *European Conference on Computer Vision*, pages 336–352. Springer, 2024. 3
- [43] Yixin Yang, Jinshan Pan, Zhongzheng Peng, Xiaoyu Du, Zhulin Tao, and Jinhui Tang. Bistnet: Semantic image prior guided bidirectional temporal feature fusion for deep exemplar-based video colorization. *IEEE Transactions on Pattern Analysis and Machine Intelligence*, 2024. 3
- [44] Junyi Zhang, Charles Herrmann, Junhwa Hur, Luisa Polania Cabrera, Varun Jampani, Deqing Sun, and Ming-Hsuan Yang. A tale of two features: Stable diffusion complements dino for zero-shot semantic correspondence. *Advances in Neural Information Processing Systems*, 36, 2024. 2, 3, 4
- [45] Lvmin Zhang, Anyi Rao, and Maneesh Agrawala. Adding conditional control to text-to-image diffusion models. In *Proceedings of the IEEE/CVF international conference on computer vision*, pages 3836–3847, 2023. 2, 3, 6
- [46] Shiwei Zhang, Jiayu Wang, Yingya Zhang, Kang Zhao, Hangjie Yuan, Zhiwu Qin, Xiang Wang, Deli Zhao, and Jingren Zhou. I2vgen-xl: High-quality image-to-video synthesis via cascaded diffusion models. *arXiv preprint arXiv:2311.04145*, 2023. 2, 3
- [47] Yuxuan Zhang, Yirui Yuan, Yiren Song, Haofan Wang, and Jiaming Liu. Easycontrol: Adding efficient and flexible control for diffusion transformer. *arXiv preprint arXiv:2503.07027*, 2025. 3, 6, 7